Review Article

ISSN 2639-9466

Nanotechnology & Applications

Fabrication of Polyaniline-Zr(IV) Molybdophosphate as a Nanocomposite and its Potential Applications

Bushra R[1,2], Khan M.A[3] and Sakdapipanich J.T[1,2*]

[1]*Department of Chemistry and Centre of Excellence for Innovation in Chemistry, Faculty of Science, Mahidol University, Bangkok, Thailand.*

[2]*Institute of Molecular Biosciences, Mahidol University, Nakorn Pathom 73170, Thailand.*

[3]*Industrial Chemistry Division, Department of Chemistry, Aligarh Muslim University, Aligarh–202002, India.*

[*]Correspondence:
Sakdapipanich J.T, Department of Chemistry and Centre of Excellence for Innovation in Chemistry, Faculty of Science, Mahidol University, Bangkok, Thailand, Fax: +66-2889-3116; Tel: +66(0)28893116; E-mail: jitladda.sak@mahidol.ac.th.

Received: 12 June 2018; **Accepted:** 06 July 2018

Citation: Bushra R, Khan M.A, Sakdapipanich J.T. Fabrication of Polyaniline-Zr(IV) Molybdophosphate as a Nanocomposite and its Potential Applications. Nano Tech Appl. 2018; 1(2): 1-8.

ABSTRACT

Electrically conductive composite material PANI- Zr(IV) molybdophosphate (PZMP) was synthesized, via treatment of Zr(IV) molybdophosphate with PANI(polyaniline) gel. The membrane of this material is fabricated for detection of mercury in waste samples. By using 4-in-line-probe the conducting behaviour of the material was determined, and it was found that conductivity of the nanocomposite lies in the range of semiconductors. The composite showed improved electrochemical properties and outstanding biological activities.

Keywords

Antimicrobial, Conducting, Nanocomposite material, Sensor.

Introduction

The composite material which was obtained by the encapsulation of conducting polymers within void spaces of inorganic host matrices has attracted a great deal of attention in the field of material science. Polymeric organic part provides mechanical and chemical stability whereas inorganic moiety enhances the electrical conductivity and thermal stability to the composite material. Synergic effect between polymer and inorganic moiety leads to their use in making accumulator and different types of sensors etc. [1-4]. Many researchers continue their efforts toward the development of organic-inorganic composite material with new properties but still this field possesses various challenges and more studies are required in order to develop practically applicable composites [5].

Now day's ion-selective electrodes with its unique characteristic properties are the most commonly-used potentiometric sensors for the detection of pollutants from the environment [6-10]. Potentiometric sensors based on organic–inorganic hybrid materials are successfully employed for the detection of various organic and inorganic contaminants from synthetic and industrial waste water samples. The composite material with its outstanding properties is the result of the contribution of two or more materials with dissimilar properties [11,12]. Most of the studies reported the utilization the composite material as electrometric sensors [13-17]. Among various conducting polymers [18-20] polyaniline is a suitable candidate because of its various technological applications [21-24]. The DC conductivity of doped composite material increases with increase in dopant level up to a certain level and then decreases. The composite material with its wide variety of applications opens new pathways in academic and industrial fields [25-28]. The present work aims in providing the productive information of polyaniline-Zr(IV) molybdophosphate (PZMP) as a nanocomposite material in diverse field.

Materials and Methods

Reagents and instruments

Monomer (aniline), initiator (potassium persulfate), Zirconium salts, molybdate salts and o-phosphoric acid were purchased from Merck. High molecular weight polyvinyl chloride powder (PVC) (M_n ~2.2x104, M_w~4.3x104) and dioctyl phthalate (DOP) (molecular weight 390.56), epoxy Resin and polystyrene were procured from Aldrich. Tetrahydrofuran (THF) and metal nitrates were obtained from Fluka. pH, potential and electrical measurements were done on Elico L 610 pH meter, digital Potentiometer EI 118 and Four in line probe (Scientific Equipment India), respectively.

Synthesis of nanocomposite material

PANI was synthesized as reported [29]. Zr(IV) molybdophosphate

was synthesized by mixing the zirconium salts (0.25M) in the aqueous solution of o-phosphoric acid and molybdate salts (0.25 M) by continuous stirring and was kept overnight for digestion. In the next step the organic-inorganic composite material was synthesized by mixing the gel of PANI with inorganic precipitate of Zr(IV) molybdophosphate via stirring and left for 24h. Afterwards, it was filtered, washed and dried at 50°C. Finally, the material was dipped in a solution of nitric acid (1.0M) for one day in order to incorporate H+ ions onto the material surface which was again filtered and dried for further studies. It is evident from Table 1 that Sample Z-2 is selected for detailed studies.

The batch method [30] was employed for the determination of distribution coefficients values of the various metal ions.

K_d = Retention of the metal ion in exchanger phase (mg/g)/ Retention of the metal ion in the supernatant solution (mg/mL) (1)

In the sorption phenomena of metal ions, H+ ions from the composite ion exchange material are exchanged with the metal ions in the solution as given below:

$$2R\text{-}H^{+} + M^{2+} \rightleftharpoons R_2M^{2+} + 2\,H^{+}$$

R= composite cation exchange material

M2+ = bivalent metal ions

As it is evident from the distribution coefficient values (Table 2) that the composite material is selective for Hg^{2+} ions because the adsorption of mercury was found to be higher as compared to that of other metal ions.

Membrane Preparation

By using different types of binding materials, numbers of membranes were fabricated. PVC membrane was prepared by grinding electroactive material and mixed with appropriate amounts of polyvinyl chloride, tetrahydrofuran and plasticizer (dioctylphthalate). The solution was mixed well and casted onto a glass dish [31] at room temperature until THF was evaporated to yield a uniform and flexible membrane. A small disc was cut from this membrane and paste on the end of the Pyrex glass tube which was later on filled with 0.1 M $Hg(NO_3)_2$ solutions.

In order to prepare the membrane of epoxy resin, a mixture of electroactive material and epoxy resin in varying amounts was prepared. This mixture was spread in between the folds of the butter paper and kept for drying overnight. The dried membrane was dipped in water in order to take away the paper from its surface.

Polystyrene based membrane was prepared by mixing desired amount of electroactive material and powdered polystyrene before being heated for 3h under a pressure of 2000 lb/in^2 in a polymer film making equipment.

S.No	Mixing Zirconium (IV) oxychloride (0.25M) (mL)	volume Sodium molybdate (0.25M) (mL)	ratio (mL) Orthophosphoric acid (0.25M) (mL)	Polyaniline (10%)	pH	Colour	Ion exchange capacity (meq g^{-1})	Weight (g)
Z-1	100	100	200	100	0.75	Green	1.1	4.3
Z-2	100	100	200	200	0.75	Green	1.3	5.3
Z-3	100	100	200	300	0.75	Green	0.99	4.2
Z-4	100	100	200	400	0.75	Green	0.67	3.4

Table 1: Preparation strategy of PZMP nanocomposite material.

Metal ions	Demineralised water	Triton X®-100 0.25%	Triton X®-100 0.50%	Triton X®-100 0.75%	Triton X®-100 1.00%	Triton X®-100 2.00%	SDS 0.25%	SDS 0.50%	SDS 0.75%	SDS 1.00%
Mg^{2+}	12	40	39	28	21	16	11	12	17	19
Zn^{2+}	09	39	37	36	25	25	14	19	21	17
Sr^{2+}	13	71	43	45	43	39	31	331	685	42
Ca^{2+}	38	03	20	31	36	77	24	24	467	54
Ba^{2+}	60	260	197	160	150	137	2450	1400	1088	425
Cd^{2+}	30	69	47	46	35	32	18	29	35	16
Cu^{2+}	95	108	89	42	42	45	39	42	56	07
Ni^{2+}	67	47	44	38	36	30	19	12	10	08
Hg^{2+}	550	1267	1260	1117	1220	1060	914	434	342	289
Al^{3+}	05	67	46	43	29	17	25	31	54	14
Fe^{3+}	23	85	81	64	58	54	11	23	50	60
La^{3+}	88	100	81	59	43	42	757	197	125	67
Er^{3+}	46	79	54	52	25	19	62	46	44	11
Th^{4+}	125	129	105	84	75	44	100	800	2900	1150
Ce^{3+}	45	50	48	46	39	12	186	494	525	137
Pr^{3+}	49	59	31	27	14	13	234	725	756	120

Table 2: K_d values of different metal ions on the column of the nanocomposite material.

EMF Measurements

EMF measurements are done by using ion selective membrane electrode consisting of ion-conducting materials. Inside the electrode resides the solution of the ion of interest at constant activity. The composition of the membrane is designed in such a manner that it yields a potential of primary ion via the mechanism of the ion-exchange.

The potential measurement is carried out using:

[Solution 2, E_{L2}] [Solution 1, E_{L1}]

Ag, AgCl | KCl (satd) || Sample solution | Membrane | Internal solution (0.1M Hg^{2+}) | Ag, AgCl

E_{L2} is the external saturated calomel electrode and E_{L1} is the internal saturated calomel electrode.

The cell emf is represented as:

$$Ecell = E_{SCE} + E_{L2} + E_m + E_{L1} - E_{SCE} \quad (2)$$

Where, E_{SCE} is the calomel electrode, E_L is the junction potential and E_m refers to the membrane potential.

The membrane potential (E_m) is expressed as:

$$E_m = \frac{RT}{Z_a F}\left[ln\,{}^{[a_A]2}/_{[a_A]1} - (Z_y - Z_a)\int_1^2 t_y\, dln\, a \pm\right] \quad (3)$$

where $[a_A]_1$ and $[a_A]_2$ are activities of counter ions, a ± signify the mean activity of electrolyte solution. A is the counter ion, Y is the co-ion, Z is the charge on the ions and t_Y symbolize the transference number of co-ions. For an ideal perm selective membrane where t_Y=0 the equation 2 is written as:

$$E_m = \pm \frac{RT}{Z_A F} \ln \frac{[a_A]2}{[a_A]1} \quad (4)$$

On combining the equation (2) and (4) we get,

$$E_{cell} = E_{SCE} - E_{SCE} + E_{L_2} + E_{L_1} \pm \frac{RT}{Z_A F} \ln[a_A]2 / \ln[a_A]1 \quad (5)$$

For cation-exchange membrane this equation is modified as:

$$E_{cell} = E_{L_2} + E_{L_1} - \frac{RT}{Z_A F} \ln[a_A]1 + \frac{RT}{Z_A F} \ln[a_A]2 \quad (6)$$

The equation (6) is rewritten [value of EL(1) and EL(2) are negligible due to the use of salt bridge]:

$$E_{cell} = [E^0] + \frac{RT}{Z_A F} \ln[a_A]2 \quad (7)$$

Nernstian slope is determined from the plotting between cell potential and log activity.

In our study all potentiometric measurements was done on digital potentiometer at room temperature (25±2°C). The parameters like response time, detection limit and pH range were evaluated.

Results and Discussion

Various samples of PZMP composite were prepared (Table 1). Sample Z-2 is selected for detailed studies. The high and low pH condition of the synthesis affects the ion exchange capacity of the material. At higher pH values there is a possibility of the oxides and hydroxides formation of metal and prepared composite would have low stability and ion-exchange capacity. In order to avoid this problem, composite material was prepared at low pH. The optimum pH for this synthesis was found to be 0.75.

As expected upon increasing the volume of anionic moiety, ion exchange capacity increases because the material has become more negatively charged and thus readily host and accommodated counter ions.

Distribution coefficient values (K_d values) were studied in two different surfactants medium. The two reported models [32-34] suitably describe the adsorption behaviour of the metal ion in the presence of the surfactant on the composite material whereas the interaction between the micelles in the bulk and at the micellar-surface is better explained by the electrostatic model. The layer that developed at micellar/solvent interface leads to the lowering of the charge density of the diffused layer and micelle due to the adsorption of the counter ions by the ionic surfactant heads on the layer. The classical electrostatic theory treats the interface as a charged surface neutralized by the counter ions [35]. From this study, it is observed that uptake of Hg^{2+} is high in both surfactants while remaining metal ions (0.1M) are poorly absorbed as shown in Table 2. SEM images at different magnifications and TEM images of the composite cation exchange material are shown in Figures 1a,b and Figure 2.

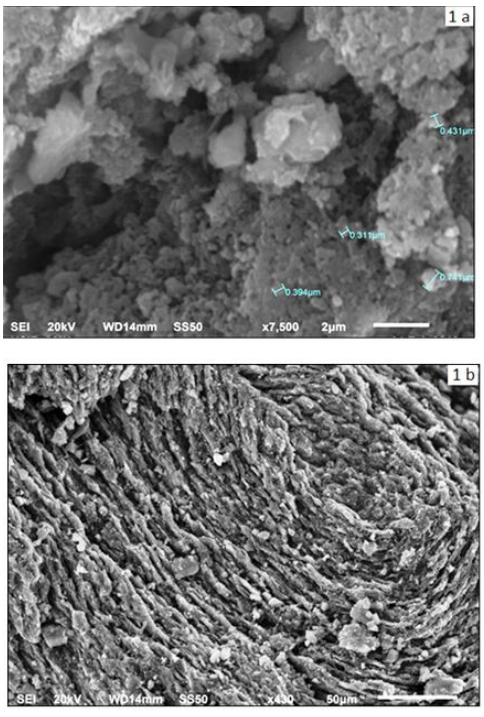

Figure 1a,b: SEM images of PZMP nanocomposite.

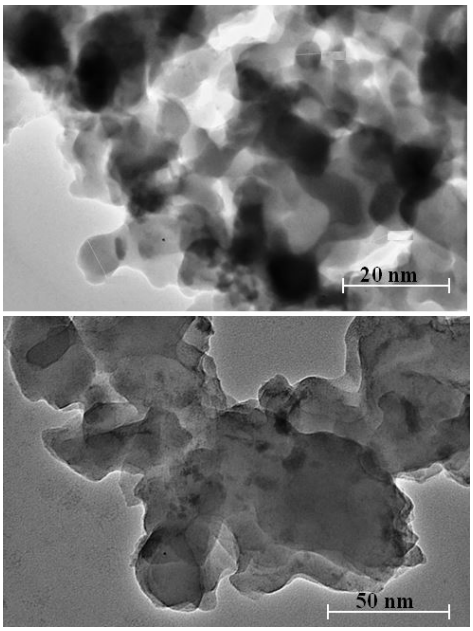

Figure 2: TEM of PZMP nanocomposite at different magnifications.

Composite ion exchange membrane has the inherent advantages of insolubility, high stability against heat and ionizing radiations as compared to inorganic and organic membranes. PVC poly(vinyl chloride) is generally used for the preparation of the membrane because this polymer have three-dimensional architecture and also provides the hydrophobic medium to ionophores, ionic sites, and ionophore complexes, so they can move freely. A PVC membrane based on hybrid ion exchange material has been utilized for the detection of Hg^{2+} ions from industrial and synthetic samples.

Membrane optimization

Nature of the ionophore and the composition of the membrane have a great influence on the sensitivity and selectivity of an ISE of the composite material. Eight different types of membrane were prepared using the composite material by mixing the ionophore (varying amount), binder (constant amount of 200mg), THF (10mL) and dioctylphthalate (66%) in a fixed amount. It is observed from Table 3 that there is no effect of the binding material on the response of the electrode. M-6 because of its quick response, reduced slope and broad concentration linear ranges is selected for detailed studies.

Electrode No.	Ionophore (mg)	Binder	Linear range (M)	Time (s)	Nerstian Slope (mV)
M1	50	Polystyrene	1.0×10^{-1} -4× 10^{-6}	12	17.7
M2	100	Epoxy resin	1.0×10^{-1}-1× 10^{-4}	20	20.0
M3	150	Epoxy resin	1.0×10^{-1}-3.5× 10^{-7}	15	18.2
M4	200	PVC	1.0×10^{-1} -1×10^{-7}	30	26
M5	250	PVC	1.0×10^{-1}-1×10^{-6}	20	28
M6	300	PVC	1.0×10^{-1}-1× 10^{-7}	15	30
M7	350	PVC	1.0×10^{-1}-1× 10^{-5}	40	23

Table 3: Optimization of membranes ingredients by varying amount of ionophore PZMP.

For conditioning, membrane electrode was placed in $Hg(NO_3)_2$ (0.1M) for seven days. Then a series of standard solutions of $Hg(NO_3)_2$ (10^{-10} M to 10^{-1} M) were prepared and their potential were measured at a fixed concentration of Hg^{2+} ion as internal reference solution. The potential response of the sensor shows linearity (1×10^{-1} to 1×10^{-7}) with a slope which is close to Nerstian value of 29.6 ± 3 mV/ concentration for bivalent cation. The detection limit was found to be 1×10^{-7}M (Figure 3), which consequently qualifies the device as a potential candidate for practical analytical applications [36].

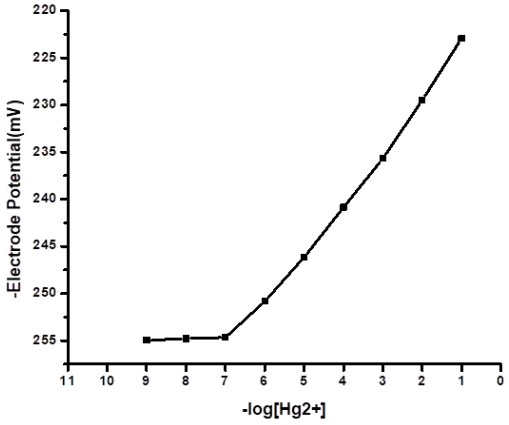

Figure 3: Calibration curve for PZMP membrane electrode.

Response time

The response time is an important parameter which measures the instant at which the metal ion solution of interest is in contact with ISE. Here the response time of the electrode of the composite material was found to be 15s (Figure 4).

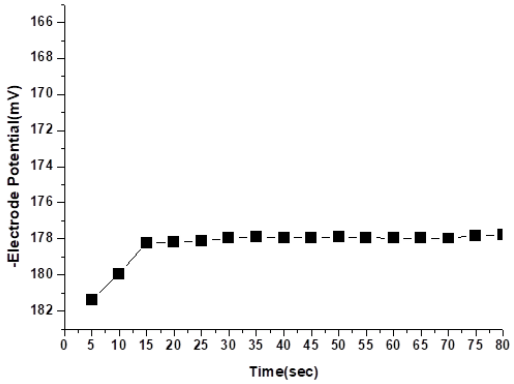

Figure 4: Electrode response at varying time intervals.

Effect of pH

To a 0.01 M of $Hg(NO_3)_2$ solution, 1 M solutions of HCl and NaOH in different volume ratios were added to prepare a series of solution in the pH range 1−12. The total volume was kept constant to 50 mL. The working pH range for this composite material is 4.0-8.0 (Figure 5).

Response of sensor towards internal solution concentration

As depicted from Figure 6, variation in the Hg^{2+} ions concentration (10^{-1} M to 10^{-3} M) does not significantly effect the response of the

electrode.

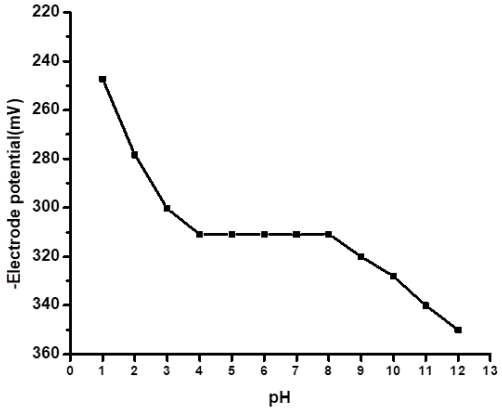

Figure 5: Electrode response at varying pH.

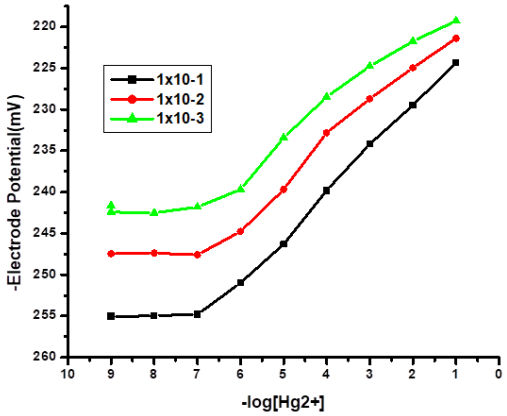

Figure 6: Electrode response towards varying internal solution concentration.

Selectivity Coefficient

Selectivity of the composite material membrane is mainly due to its ion recognition properties of the electro-active material (i.e. it binds the ion of interest leaving the other co-ions behind). In the present work the ISE is selective for Hg^{2+} ions and thus a membrane potential is developed when H^+ on the membrane surface is exchanged with the Hg^{2+} ions. The selectivity coefficients value depends on the selectivity of the electrode. The greater the value of selectivity coefficient the lesser the selectivity of the electrode is. The selectivity coefficient (K_{ij}) has been introduced in the Nikolski-Eisenman equation, which gives information about the electrode response towards the primary and interfering ions in a mixture.

$$E = E^0 + \left(2.303\frac{RT}{Z_i F}\right)\log(a_i + K_{i_j} a_j \frac{z_i}{z_j} \quad (8)$$

where E and E° is the potential and standard potential of the electrode, respectively; ai and aj , are the activity of i and j ions and Zi and Zi are the charge of i and j ions, respectively. Kijpot is the selectivity coefficient of the electrode.

In the present study, mixed solution method MSM [37] was used for determining the selectivity coefficient by using the equation:

$$K_{i_j}^{pot} = \log[10^{\left(Ei+j-\frac{E_i}{m}\right)} - z_i / Z_j \log a_j \quad (9)$$

where i, j, are the activities and Zi and Zj are charges of the primary and interfering ions, respectively. The selectivity coefficient well defined the extent of the interference of foreign ion (M^{n+}) with the primary ions. The selectivity coefficient values were calculated as shown in Table 4 clearly indicated that there is no affect on the selectivity of the electrode by the interference of foreign ions.

Interfering ions	Selectivity coeffecients
Cu^{2+}	4.0× 10-5
Mg^{2+}	3.5× 10-4
Cd^{2+}	4.9× 10-4
Fe^{3+}	3.7× 10-2
Mn^{2+}	2.1× 10-4
Na^{+}	4.7× 10-7
K^{+}	8.5× 10-4

Table 4: Values of selectivity coefficients of different interfering ions.

As it is evident from Table 5 that the overall performance of the present sensor is better than other Hg^{2+} selective electrode reported in literature [38-46].

Membrane sample	Range of concentration (M)	Response time (s)	Slope Reference (mV)
Calixarene derivative	5.0×10^{-6}- 5×10^{-2}	20	28.7 [38]
2-Mercaptobenzimidazole	1.0×10^{-6}-1×10^{-1}	20-100	28.5 [39]
1,2-bis-(N'-benzoylthioureido) cyclohexane	1.0×10^{-6}-1×10^{-1}	20-100	29 [40]
1,3-diphenylthiourea	6.0×10^{-6}-5×10^{-4}	20	30.8 [41]
Calix[2]thieno[2]pyrrole	1.0×10^{-6}-1×10^{-2}	20	27.8 [42]
PANI-Sn(IV)phosphate	1.0×10^{-6}-1×10^{-1}	14	40 [43]
DQDC	0.005mM-1mM	-	25.8 [44]
Salicylaldehyde thiosemicarbazone	1.7×10^{-6}-1×10^{-1}	30	29 [45]
2- MBI	1.0×10^{-7}-1×10^{-2}	33	29.1 [46]
Proposed assembly	1.0×10^{-7}-1×10^{-1}	15	30 This work

Table 5: Comparative study of various mercury selective electrodes.

Application of the proposed sensor

The potentiometric titration of Hg^{2+} ion with EDTA demonstrated the practical utility of the proposed sensor as an indicator electrode. On addition of EDTA to $Hg(NO_3)_2$ solution (portion of 5 mL) at pH 4 buffered by acetate buffer, it was found that electrode potential decreases due to the complexation of free Hg^{2+}ion with EDTA (Figure 7).

The waste samples was first filtered through Millipore cellulose membrane and then dissolved in nitric acid of appropriate normality and then subjected to pre-concentration [47]. After that the amount of the metal ion was determined by Flame atomic absorption spectroscopy (FAAS). The concentration of the mercury in the samples was also determined by using the proposed sensor for comparison. The data is summarized in Table 6. The results are in good agreement with those obtained from the atomic absorption spectrometry method.

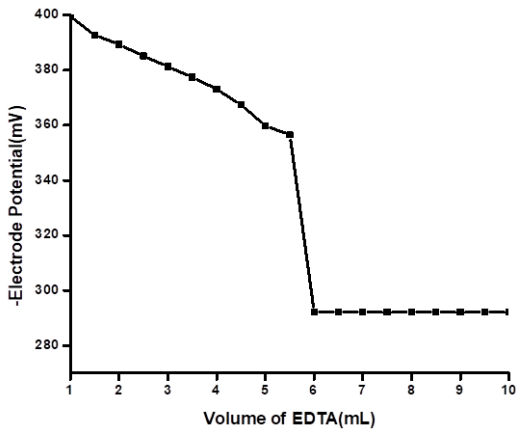

Figure 7: Potentiometric titration curve using PZMP-PVC membrane electrode.

Samples	Method	Amount of Hg^{2+} found* (μgL^{-1}) (%RSD)[a]
B_1	Membrane electrode assembly AAS	12.27(0.07) 12.50 (0.05)
B_2	Membrane electrode assembly AAS	14. 80(0.04) 15.0 (0.02)

Table 6: Analysis of water samples containing mercury using proposed method and that of the AAS.

[a]% RSD, Relative standard deviation.

Conclusion

Developed potentiometric sensor exhibits Nernestian sensitivity with a detection limit of 1.0×10^{-7} M and response time of 15s. The developed ion selective membrane electrode has been successfully utilized for the analyses of Hg^{2+} ions from real and synthetic samples with high accuracy and precision. From electrical conductivity, measurements and antimicrobial studies, it was confirmed that PZMP as the nanocomposite can be used as a semiconductor and also as an antimicrobial agent.

Acknowledgments

The authors would like to acknowledge Mahidol University for the main financial supports through the Postdoctoral Fellowship Program # MU-PD-2017-7, # MU-PD-2018-8 and the Center of Excellence for Innovation in Chemistry, Commission on Higher Education (PERCH-CIC). We also appreciated for collaboration with Aligarh Muslim University.

Grant Details

The authors would like to acknowledge Mahidol University Postdoctoral Fellowship Program for the financial support through the Postdoctoral Fellowship Program # MU-PD-2017-7, # MU-PD-2018-8.

References

1. Huang J, Virji S, Weiller BH, et al. Nanostructured polyaniline sensors. Chem Eur J. 2004; 10: 1314-1319.
2. Anilkumar P, Jayakannan M. Hydroxyl-Functionalized Polyaniline Nanospheres: Tracing Molecular Interactions at the Nanosurface via Vitamin C Sensing. Langmuir. 2008; 24: 9754-9762.
3. Yufeng M, Ali SR, Dodoo AS, et al. Enhanced Sensitivity for Biosensors: Multiple Functions of DNA-Wrapped Single-Walled Carbon Nanotubes in Self-Doped Polyaniline Nanocomposites. J Phys Chem B. 2006; 110: 16359-16365.
4. Hatchett DW, Josowicz M. Composites of Intrinsically Conducting Polymers as Sensing Nanomaterials. Chem Rev. 2008; 108: 746-769.
5. Guerrini A, Romano G, Carosi L, et al. Cost Savings in Wastewater Treatment Processes: the Role of Environmental and Operational Drivers. Water Resour Manage. 2017; 31: 2465-2478.
6. Dimeski G, Badrick T, John AS. Ion Selective Electrodes (ISEs) and interferences-a review. Clin Chim Acta. 2010; 411: 309-317.
7. Arida HA, Ahmed MA, El-Saied AMA. A Novel Coated Graphite Rod Th(IV) Ion Selective Electrode Based On Thorium Oxinate Complex and Its Application. Sensors. 2003; 3: 424-437.
8. Huang MR, Gu GL, Ding YB, et al. Advanced Solid-Contact Ion Selective Electrode Based on Electrically Conducting Polymers. Chin J AnalChem. 2012; 40: 1454-1460.
9. Arida HA, Al-Hajry A, Maghrabi IA. A Novel Solid State Copper (II) Thin Film Micro Sensor Based on Organic Membrane and Titanium Dioxide Nano Composites. Int J Electrochem Sci. 2014; 9: 426-434.
10. Arida HA, Kloock JP, Schöning MJ. Novel Organic Membrane-based Thin-film Microsensors for the Determination of Heavy Metal Cations. Sensors. 2006; 6: 435-444.
11. Nabi SA, Naushad Mu, Bushra R. Synthesis and characterization of a new organic-inorganic Pb2+selective composite cation exchanger acrylonitrile stannic (IV) tungstate and its analytical applications. Chem Eng J. 2009; 152: 80-87.
12. Nabi SA, Bushra R, Naushad Mu, et al. Synthesis, characterization and analytical applications of a new composite cation exchange material poly-o-toluidine stannic molybdate for the separation of toxic metal ions. Chem Eng J. 2010; 165: 529-536.
13. Wei Y, Fang F, Yang W, et al. Preparation of a Nitrite Electrochemical Sensor Based on Polyaniline/Graphene Ferrocenecarboxylic Acid Composite Film Modified Glass Carbon Electrode and its Analytical Application. J Braz Chem Soc. 2015; 26: 2003-2013.
14. Arfin T, Bushra R, Mohammad F. Electrochemical sensor for the sensitive detection of o-nitrophenol using graphene oxide-poly (ethyleneimine) dendrimer-modified glassy carbon electrode. Graphene Technol. 2016; 1: 1-15.
15. Salavagione HJ, Díez-Pascual AM, Lázaro E, et al. Chemical sensors based on polymer composites with carbon nanotubes and graphene: the role of the polymer. J Mater Chem A. 2014; 2: 14289-14328.
16. Rahman MM, Khan A, Asiri AM. Chemical sensor development based on poly (o-anisidine) silverized–MWCNT nanocomposites deposited on glassy carbon electrodes for environmental remediation. RSC Adv. 2015; 5: 71370-71378.

17. Omar FS, Duraisamy N, Ramesh K, et al. Conducting polymer and its composite materials based electrochemical sensor for Nicotinamide Adenine Dinucleotide (NADH). Biosens Bioelectron. 2016; 79: 763-775.
18. Stenger-Smith JD. Intrinsically electrically conducting polymers. Synthesis, characterization, and their applications. Prog Polym Sci. 1998; 23: 57-59.
19. Shirakawa H. The discovery of polyacetylene film-the dawning of an era of conducting polymers. Synthetic Met. 2001; 125: 3-10.
20. Heeger AJ. Semiconducting and metallic polymers: the fourth generation of polymeric materials. Synthetic Met. 2002; 125: 23-42.
21. Patil SD, Raghavendra SC, Revansiddappa M, et al. Synthesis, transport and dielectric properties of polyaniline/Co3O4 composites. B Mater Sci. 2007; 30: 89-92.
22. Li C, Shi G. Synthesis and electrochemical applications of the composites of conducting polymers and chemically converted graphene. Electrochim Acta. 2011; 56: 10737-10747.
23. Chen Y, Xu C, Wang Y. Viscoelasticity behaviours of lightly cured natural rubber/zinc dimethacrylate composites. Polym Compos. 2012; 33: 1206-1214.
24. Bushra R, Naushad Mu, Adnan R, et al. Polyaniline supported nanocomposite cation exchanger: Synthesis, characterization and applications for the efficient removal of Pb2+ ion from aqueous medium. J Ind Eng Chem. 2015; 21: 1112-1118.
25. Vatutsina OM, Soldatov VS, Sokolova VI, et al. A new hybrid (polymer/inorganic) fibrous sorbent for arsenic removal from drinking water. React. Funct Polym. 2007; 67: 184-201.
26. Bushra R, Shahadat M, Nabi SA, et al. Synthesis, characterization, antimicrobial activity and applications of composite adsorbent for the analysis of organic and inorganic pollutants. J Hazard Mater. 2014; 264: 481-489.
27. Bushra R, Shahadat M, Khan MA, et al. Optimization of Polyaniline Supported Ti(IV) Arsenophosphate Composite Cation Exchanger Based Ion-selective Membrane Electrode for the Determination of Lead. Ind Eng Chem Res. 2014; 53: 19387-19391.
28. Shahadat M, Nabi SA, Bushra R, et al. Synthesis, characterization, photolytic degradation, electrical conductivity and applications of nanocomposite adsorbent for the treatment of pollutants. RSC Adv. 2012; 2: 7207-7220.
29. Nabi SA, Bushra R, Shahadat M, et al. Development of nano-composite adsorbent for removal of metals from industrial effluent and synthetic mixtures; its conducting behavior. Desalination. 2012; 289: 1-11.
30. Nabi SA, Bushra R, Naushad Mu. Synthesis, Characterization and analytical applications of a new composite cation exchange material Acetonitrile stannic (IV) selenite: Adsorption behaviour of toxic metal ions in nonionic surfactant medium. Sep Sci Technol. 2011; 46: 847-857.
31. Craggs A, Moody GJ, Thomas JDR. PVC matrix membrane ion-selective electrodes. Construction and laboratory experiments. J Chem Educ. 1974; 51: 541-544.
32. Mazer NA, Benedek B, Carey MC. An investigation of the micellar phase of sodium dodecyl sulfate in aqueous sodium chloride solutions using quasielastic light scattering spectroscopy. J Phys Chem. 1976; 80: 1075-1085.
33. Misse PJ, Mazer NA, Benedek GB, et al. Thermodynamic analysis of the growth of sodium dodecyl sulfate micelles. J Phys Chem. 1980; 84: 1044-1057.
34. Porte G, Appell J. Growth and size distributions of cetylpyridinium bromide micelles in high ionic strength aqueous solutions. J Phys Chem. 1981; 85: 2511-2519.
35. Gunnarsson G, Jonsson B, Wennerstrom H. Surfactant association into micelles. An electrostatic approach. J Phys Chem. 1980; 84: 3114-3121.
36. Demirel A, Canel DE, Shahabuddin. Hydrogen Ion-Selective Poly (vinyl chloride) Membrane Electrode Based on a p-tert-Butylcalix[4]arene –oxacrown-4. Talanta. 2004; 62: 123-129.
37. Reiliy CN, Schmidt RW, Sadek FS. Chelon approach (I) survey of theory and application. J Chem Edu. 1959; 36: 555-564.
38. Lu J, Tong X, He X. A mercury ion-selective electrode based on a calixarene derivative containing the thiazole azo group. J Electroanal Chem. 2003; 540: 111-117.
39. Mazloum M, Amini MK, Baltork IM. Mercury selective membrane electrodes using 2-mercaptobenzimidazole, 2-mercaptobenzothiazole, and hexathiacyclooctadecane carriers. Sens. Actuators B. 2000; 63: 80-85.
40. Jumal J, Yamin MB, Ahmad M, et al. Mercury Ion-Selective Electrode With Self-plasticizing Poly(n–buthylacrylate) Membrane Based On 1,2-Bis-(N'–benzoylthioureido) cyclohexane As Ionophore. APCBEE Procedia. 2012; 3: 116-123.
41. Pérez-Marín L, Otazo-Sánchez E, Macedo-Miranda G, et al. Mercury(II) ion-selective electrode. Study of 1,3 diphenylthiourea as ionophore. Analyst. 2000; 125: 1787-1790.
42. Abbas II. Mercury (II) Selective Membrane Electrode Based on Calix [2] thieno [2] pyrrole. Int J Chem. 2012: 4: 23-29.
43. Khan AA, Inamuddin. Applications of Hg(II) sensitive polyaniline Sn(IV) phosphate composite cation-exchange material in determination of Hg2+ from aqueous solutions and in making ion-selective membrane electrode. Sens. Actuators B. 2006; 120: 10-18.
44. Sihombing E, Situmorang M, Sembiring T, et al. The Development Of Mercury Ion Selective Electrode With Ionophore 7, 16-Di-(2-Methylquinolyl)-1,4,10, 13-Tetraoxa-7,16-Diazacyclooctadecane (DQDC). Mod App Sci. 2015; 9: 81-90.
45. Mahajan RK, Kaur I, Lobana TS. A mercury (II) ion selective electrode based on neutral salicylaldehyde thiosemicarbazone. Talanta. 2003; 59: 101-105.
46. Han WS, Wi KC, Park WS, et al. Mercury Ion Selective Poly(aniline) Solid Contact Electrode Based on 2-Mercaptobenzimidazol Ionophore. Russ J Electrochem. 2012; 48: 525-531.
47. Islam A, Ahmad A, Laskar MA. Flame Atomic Absorption Spectrometric Determination of Trace Metal Ions in Environmental and Biological Samples after Preconcentration on a Newly Developed Amberlite XAD-16 Chelating Resin

Containing p-Aminobenzene Sulfonic Acid. J AOAC Int. 2015; 98: 165-175.
48. Bushra R, Arfin T, Oves M, et al. Development of PANI/MWCNTs decorated with cobalt oxide nanoparticles towards multiple electrochemical, photocatalytic and biomedical application sites. New J Chem. 2016; 40: 9448-9459.
49. Alam M, Ansari AA, Shaik MR, et al. Optical and electrical conducting properties of Polyaniline/Tin oxide nanocomposite. Arabian J Chem. 2013; 6: 341-345.
50. Bushra R, Shahadat M, Khan MA, et al. Preparation of polyaniline based nanocomposite material and their environmental applications. Int J Environ Sci Technol. 2015; 12: 3635-3642.

Supplementary Material

Investigation of biological activity

The mechanism of antibacterial activity involves the binding of the composite to the bacterial cell by rupturing the bacterial cell wall. This binding is responsible for the cell membrane disruption by the decomposition of the functional groups on the surface of the cell membrane.

The antibacterial activity of composite material was tested by using well-diffusion method against P. dispersa P. aeruginosa, B. thuringiensis and S. aureus and compared with drug Ampicillin [48]. In a flask, different amount of the testing material and sterilized nutrient broth culture of actively dividing bacterial cells of about 106 CFU/mL was inoculated, and shaked at the speed of 160 rpm in an orbital shaker. The growth of the bacteria was monitored visually and spectrophotometrically.

The test material has excellent antimicrobial activity in terms of zone of inhibition (ZOI) towards the strains of gram positive and negative bacteria. For B. thuringiensis composite material developed a 26 mm zone of inhibition and for S. aureus, P. aeruginosa, P. dispersa values was found to be 24nm, 23nm and 20nm, respectively. Minimum MIC of 45 µg/mL was found against B. thuringiensis and maximum against P. dispersa (MIC of 60 µg/mL).

Conductivity measurements

In order to perform the conducting studies, the material was treated with HCl (0.1 M) and washed with demineralized water and then dried at 50°C for 24 hrs. With the help of the hydraulic press at a pressure of 25 kN, pellets of this dried material (300 mg) were developed for conductivity measurements. All conductivity measurements were performed on a 4-in-line-probe in temperature range between 30 and 200 °C. The following equations are employed for the conductivity measurements:

$\sigma = \sigma 0 / G7 (W/S)$

$G7 (W/S) = \ln 2 (2S/W)$

$\sigma 0 = 2\pi S (V/I)$

where σ, G7 (W/S), S, I and V are the conductivity (S cm-1), correction factor (function of thickness of the sample) probe spacing (cm), current (A) and voltage, respectively.

From the results of conductivity measurements, it can be concluded that conductivity of the material increases with temperature. This implies the characteristic of a nanocomposite as a semiconductor (Figures S-1 and S-2). The factors that are involved in the enhancement of conductivity are the presence of the charge carriers and the orientations of polymer chains for electron delocalization [49] in the system. Like other semiconductors, this nanocomposite material follows the Arrhenius model [50]. By varying the percentage of the inorganic precipitate (Figure S-3) the conductivity increases with a maximum value at 15%, after that there is a decrease (Xu et al. 2005; Su and Kuramoto 2000). At 50 and 80°C conductivity was quite stable, but with further increase in temperature, there is a decrease in conductivity which reveals that composite material followed the Arrhenius equation (Figure S-4).